Preliminary Evaluation of the Airborne Imaging Spectrometer for Vegetation Analysis

by

Alan H. Strahler
Curtis E. Woodcock
Department of Geology and Geography
Hunter College
City University of New York

Final Report: Phase I

March 1984

This report was prepared for the Jet Propulsion Laboratory, California Institute of Technology, sponsored by the National Aeronautics and Space Administration.

Introduction

The purpose of this report is to document the experiences and results associated with Phase One of a project entitled "Preliminary Evaluation of the Airborne Imaging Spectrometer for Vegetation Analysis." The primary goal of the project was to provide ground truth and manual interpretation of data from an experimental flight of the Airborne Infrared Spectrometer (AIS) for a naturally vegetated test site. Two field visits were made; one trip to note snow conditions and temporally related vegetation states at the time of the sensor overpass, and a second trip following acquisition of prints of the AIS images for field interpretation. Unfortunately, our ability to interpret the imagery was limited by the quality of the imagery due to the experimental nature of the sensor.

Background

The scientific basis of remote sensing of earth resources is that different substances reflect (or emit) radiation with different intensities in different regions of the electromagnetic spectrum (EMS). To date, remote sensing from spacecraft has been dominated by the analysis of radiance data integrated over broad bands of the EMS. The most common data available are from the Landsat Multispectral Scanner (MSS), which has three spectral bands

100nm wide, and one spectral band 300nm wide. Due to the small number of bands and their coarse spectral resolution, much work in remote sensing has centered on statistical information extraction techniques, rather than an improved understanding of reflectance spectra and their resulting radiance spectra.

A newer sensor, the Thematic Mapper (TM) presents an improvement, providing six bands of data from the visible to the shortwave infrared (the thermal band is not considered here). However, these bands are still relatively broad, ranging from 70nm at 0.45um to 270nm at 2.08um. While this sensor is an improvement over the MSS, its band width severly limits the analysis of reflectance spectra. Preliminary indications are that the analysis of TM data will continue along the lines of statistically-based empirical procedures similar to those used with MSS data.

The AIS measures reflected radiance over the near infrared portion of the EMS from 1.2 to 2.4um. For the flight of our Goosenest study area, the AIS was configured to collect 32 bands approximately 10nm wide in one of four wavelength regions: 1.2-1.5um, 1.5-1.8um, 1.8-2.1um, and 2.1-2.4um. For each of two test sites, three overpasses were made to collect data in each of these wavelength regions except the 1.8-2.1um region which was omitted due to expected atmospheric water vapor absorption. In

addition to the AIS, 35mm photography and video cassettes of the flightline were taken during the overpass to help with future analysis. The data from only one test site was processed and sent to the investigators.

Field Visit 1

The first field visit occurred immediately following the overpass of the AIS and was considered essential to note the phenological state of the various plant species, and also note the extent of snow cover. Snow cover was expected to be unimportant at the time the original proposal was submitted, but due to record snowfall in 1983 it was necessary to know which features in the imagery would be attributable to snow.

Due to the narrow swath width of the AIS (900m), it was important to determine the flight path for each overpass of the study area. At NASA Ames immediately following the return of the C-130, the video tapes of the overpasses were studied and a line approximating the center of each overpass was sketched on 1:24000 color air photos for use in the field. These lines were helpful in limiting the area requiring ground truth, but may not have been as accurate as might normally be possible due to oil that accidentally covered the lens of the video camera during the flight. The data from the AIS and the 35mm camera

were not available for this field visit because of the processing required prior to their use.

During the field visit, various areas along each flightline were visited, and detailed notes about the vegetation at the sites were made. In addition, 35mm slides using standard color film, and color infrared film were taken. These photographic slides serve two purposes: 1) to document the site at the time of the overpass, and 2) to give a preliminary indication of variable reflectance of vegetation between the visible and near infrared wavelengths. These photographs are only capable of providing an initial indication because the color infrared film is sensitive to different wavelengths than the AIS.

The first test site, referred to as the "Grass Lake" site, runs along a northeast-southwest orientation. At the southwest end is Herd Peak and an interesting gradient of tree species. At the highest elevation, red fir is the dominant tree species, giving way down slope to a mixed conifer forest that is often dominated by white fir. Other tree species common in this mixed conifer area are incense cedar, Douglas fir, and ponderosa and Jeffery pine. The species variety in this location could allow interesting investigation of variable reflection of coniferous tree species. Figures 1a and 1b are color and color infrared prints of a mixed conifer stand in the Herd

Peak area. The tallest tree is a Douflas fir and the two shorter trees to the left are a white fir and a ponderosa pine (far left).

Below Herd Peak in the transect is Grass Lake, which is a fairly large lake (approximately 3 miles long) but very shallow. In fact, at certain times of the year the lake is almost dry. As a result, there are interesting patterns of different species of grasses that grow throughout the lake and along its shore, providing considerable variety for spectral differentiation. Figures 2a and 2b show a general view of Grass Lake from the southwest, pointing approximately in the direction of the AIS overpass. At the time of the overpass the Lake was relatively full due to the high precipitation levels in the winter. The white areas in the Lake are dead grasses killed by high water levels. Figures 3a and 3b were taken from the Lake's edge and show the variety of grasses common around the Lakes's border. Several distinct zones of grasses are visible descending from the dry shoreline into the shallow waters along its edge.

Northeast of Grass Lake is an area that is basically flat and has vegetative types similar to high desert habitats. The area is characterized by sparsely stocked ponderosa and Jeffery pine and an extensive understory of brush comprised of antelope bush (purshia tridentata)

(shown in figure 4a and 4b), manzanita (Arctostaphylos spp.), great basin sage (Artemisia tridentata), and rabbit brush (Chrysothamnus spp.). In addition, there are several lava flows in the area that are distinctively marked by dense patches of mountain mahogany (Cercoarpus betuloides) that grow along their margins. Figures 5a and 5b show a typical mix of brush and sparse pines in the northeast portion of the Grass Lake transect.

The second test site runs in a north-south direction and is considerably east of the Grass Lake test site. We refer to this test site as the "Dock Well" area, and it has two distinctive sections. The northern section is very flat and is similar to the "high desert" area described in the Grass Lake site in that it is sparsely stocked with ponderosa and Jeffery pine. However, the understory brush in this test site grows considerably lower and tends to be more spatially homogeneous. As a result, this area gives a close approximation to a simple model of individual trees on a homogeneous background. A simple scene such as this has proved useful in past exploratory research where the number of convolving factors are minimized. In addition, SPOT simulator data of this area was collected later in the summer, which could lead to some interesting comparisons of datasets. Figure 6a and 6b show the general appearance of the flat northern

section of the Dock Well test site.

The second part of the Dock Well site is a long, gentle hillslope that leads to a ridge at the extreme southern end of the site. There is a gradual change in tree species composition as elevation increases. At the bottom of the slope the area is similar to the high desert area previously described. As elevation increases the forest canopy becomes more dense, the trees become bigger, and some white fir is present. Eventually white fir becomes dominant, incense cedar is present, and the pines become more scarce. At the highest elevations, red fir becomes the dominant species with white fir still present but less frequent. This gradation of tree species is expected to afford an interesting opportunity to explore the spectral reflectance of different conifer species. Figures 7a and 7b show three tree species in the mixed conifer area of the test site. The tall trees in the back are ponderosa pine, the tree in the front left is incense cedar, and the tree in the front right is white fir. Subtle differences in the tone in both the color and infrared prints can be seen for the different tree species, suggesting the possibility of different reflectance spectra for these species throughout both the visible and near infrared portion of the EMS.

Second Field Visit

Prior to the second field visit, we received the roll of negatives from the 35mm camera and had 8x10 prints made of each frame. The AIS data were not received until we were in the field. The data only included the Dock Well site and consisted of three large prints for each of the three passes over the site (one for each grating position). It was unfortunate that the data from the Grass Lake site were unavailable, as this site has the most obvious features and would have been the easier of the two sites on which to begin work. Also, there was no snow in this test site at the time of the overpass.

Considerable time was required to determine how the prints for each grating position fit together. Problems arose due to the generally poor quality of the data and due to the fact that the data for each print had been processed separately. This problem resulted in the areas of overlap on adjoining prints being very difficult to recognize. This problem is readily apparent when the overlapping areas of Figure 8a 8b and 8c are compared. We would strongly recommend in the future that the data from a single grating position all be processed identically. Another problem related to the separate processing of different parts of a single flightline is the dark banding found in some parts of the data. Since this banding does

not occur uniformly throughout single flightlines and is confined to individual prints, it is assumed to be an artifact of the image processing.

There are a couple of additional suggestions we would like to make regarding the processing of the data. First, the use of Gaussian stretches may not be advisable because they tend to concentrate a large number of the pixels in the middle gray tones, limiting the contrast in the image. The images might be more easily interpreted following an equal area stretch or another similar technique. A second suggestion concerns spectral filtering. Spectral filtering for the replacement of missing values makes sense for this imagery, but any broad spectral filtering based on a running means algorithm (averaging with equal weights for all pixels used) rather than methods that weight the contribution to the output value as a function of their distance can produce artifacts in the resulting spectra (Holloway 1958).

While the quality of the prints was poor, and the features they exhibited were puzzling and confusing, we were nonetheless able to locate two areas on the ground that showed interesting characteristics on the AIS imagery. The first of these was a cinder cone, which is visible on the AIS print as a group of three related crescent shapes at the 1.5um end of the image, and as a

rounded form at the 1.8um end (Figure 9a and 9b). Field reconnaissance of the cone revealed three types of ejecta present at the surface: red, black, and white (Figures 10a and 10b). Representative sample of each type of rock were collected and sent to JPL in the fall of 1983.

An examination of accompanying Nikon camera photographics of the cinder cone shows most of the cone was covered by snow at the time of the overpass. The crescentic shapes at the 1.5um end of the AIS image are simply areas of ejecta that are not snow covered. Since snow absorbs in the shorter wavelengths in this region, it appears dark on the AIS image. At the longer wavelengths of the AIS image, the conical shape is much better revealed. Further, there appear to be subtle differences in shading between light and medium grey tones that correspond roughly to the distribution of red and black ejecta, as compared to the lighter-colored pyroclastic materials. Since these materials were obscured by snow, this relation may be artifactual, or coincidentally related to the topography. We are unaware of whether or not there is significant penetration of snow by light at these wavelengths to allow actual sensing of the surface.

Another interesting area taken from the 1.5-1.8um image that we were able to identify on the ground is shown in Figure 11. As the accompanying panchromatic photo

(Figure 12) shows, the feature is not spectrally distinguishable in the visible. However, it presents a high reflectance (bright aspect) in the shortwave infrared. Ground reconnaissance (Figures 13a and 13b) revealed this area as a very recent clearcut, in which the ground surface had been disturbed and the logging slash had been piled for burning using heavy equipment. Although the preprocessing of the AIS imagery leaves us somewhat uncertain as to whether or not light tones indicate high reflectance, the scarified soil suface is quite distinctive.

A Second Overpass of the AIS

Following improvements of the AIS, a second overpass of both the Grass Lake and Dock Well test sites was flown. On January 12th, we visited JPL and received tapes containing the imagery for both sites, and contact prints of the Nikon 35mm photography. In addition, we were briefed on recent developments in image processing software designed for analysis of data from the AIS.

During our visit, we also spent some time looking at the imagery from the new flight on the interactive display monitor. It was readily apparent that the quality of the new flight was far superior to the original data we had examined. The improved quality of the imagery was

encouraging, as this data will be used in Phase II of this project, which involves digital analysis of AIS data. While we were looking at the AIS imagery, we used the new JPL software to plot spectra of several forest species for Grating Position 0 (1.5-1.8um) and 1 (1.8-2.1um). While these graphs should not be interpreted as true "reflectance spectra" because there is no correction for variation in available radiance at different wavelenths or atmospheric effects, they show some interesting features that can be pursued in the next phase of this project.

The most obvious feature in the graph for Grating Position 0 (Figure 14) is the variation in the overall magnitude of reflectance for the four areas analyzed. In addition, the shapes of the graphs for each area show some subtle, but possibly important differences. Two peaks in reflectance for each area can be seen; the first one near 1.59um and the second near 1.65um. Interestingly, the second peak for the ponderosa pine areas is more pronounced and occurs one spectral band (approximately 10nm) earlier than in the plots for the mixed conifer and red fir areas. Also, in the region 1.52-1.57um the mixed conifer and red fir plots are considerably flatter than the ponderosa pine plots.

In the spectral plots for Grating Position 1 (Figure 15), again the most obvious feature is the general

difference in the magnitude of reflectance between some of the forest areas. However, in this graph two sites, one mixed conifer and one red fir, have almost identical plots. The ponderosa pine area has markedly higher reflectance than the other areas. The variation in shapes of the plots is even more subtle than in Grating Position 0. The small drop in reflectance at about 2.09um in one red fir and the ponderosa pine area might be important, as could be the sudden jump in reflectance at 2.05um for the red fir and mixed conifer sites.

While these differences seem slight, only further investigation will determine which of these, and other unnoticed differences are important. It should be remembered that these graphs are for areas that characterize very similar conifer species, and no attempt has been made to compare these graphs with different vegetation types. These graphs are very exciting because very little is known about vegetative reflectance in the near infrared.

References

Holloway, J. L., 1958. Smoothing and Filtering of Time Series and Sapce Fields, Advances in Geophysics, vol 4, p 351-389.

Figure 1a.

Figure 1b.

Figures 1a and 1b are color and color infrared prints of a mixed conifer stand in the Grass Lake test site. The tall tree in back is a Doulgas Fir, with a wh't. fir and a ponderosa pine in the left side of the pict.

Figure 2a.

Figure 2b.

Figures 2a and 2b are color and color infrared prints of Grass Lake. Notice the variations in depth of the Lake and patterns of dead and healthy grasses in the middle of the Lake and along its edge.

Figure 3a.

Figure 3b.

Figures 3a and 3b are color and color infrared prints of an area along the edge of Grass Lake. Notice the zones of different grasses and their variation in reflectance in both the visible and near infrared wavelengths.

Figure 4a.

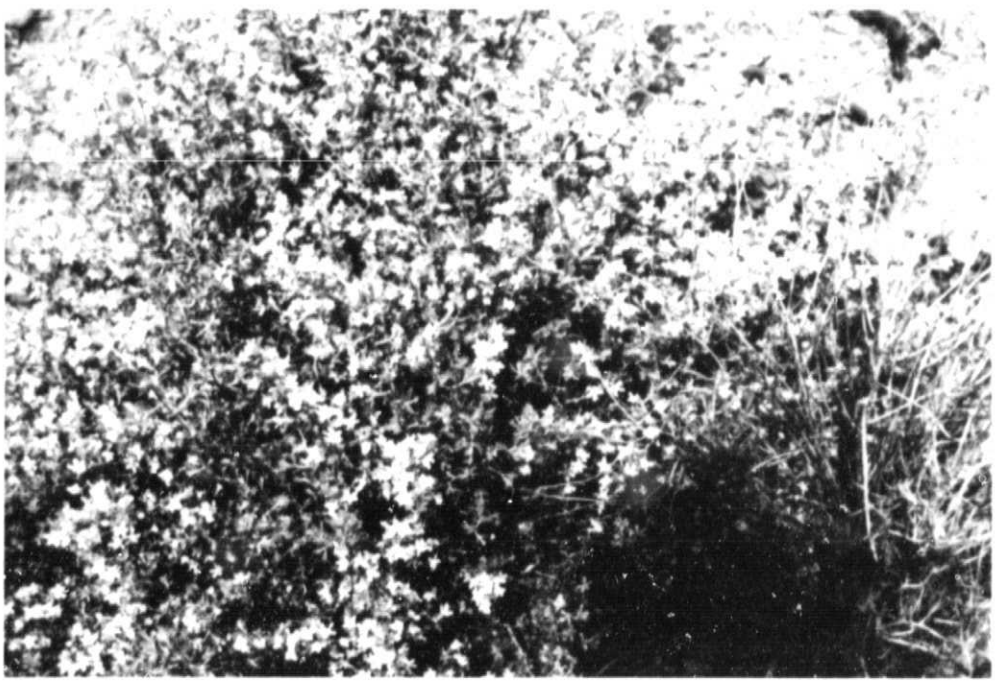

Figure 4b.

Figures 4a and 4b are color and color infrared prints of antelope bush (Purshia tridentata).

Figure 5a.

Figure 5b.

Figures 5a and 5b are color and color infrared prints of the general mix of brush and trees characteristic of the northeast portion of the Grass Lake test site. Notice the variation in reflectance between brush species and between the trees and the brush.

Figure 6a.

Figure 6b.

Figures 6a and 6b are color and color infrared prints of the northern section of the Dock Well test site.

Figure 7a

Figure 7b

Figures 7a and 7b are color infrared prints of three tree species in the mixed conifer area of the Dock Well test site. The two big trees in back are ponderosa pine, with a small incense cedar in the lower left, and a small white fir in the lower right.

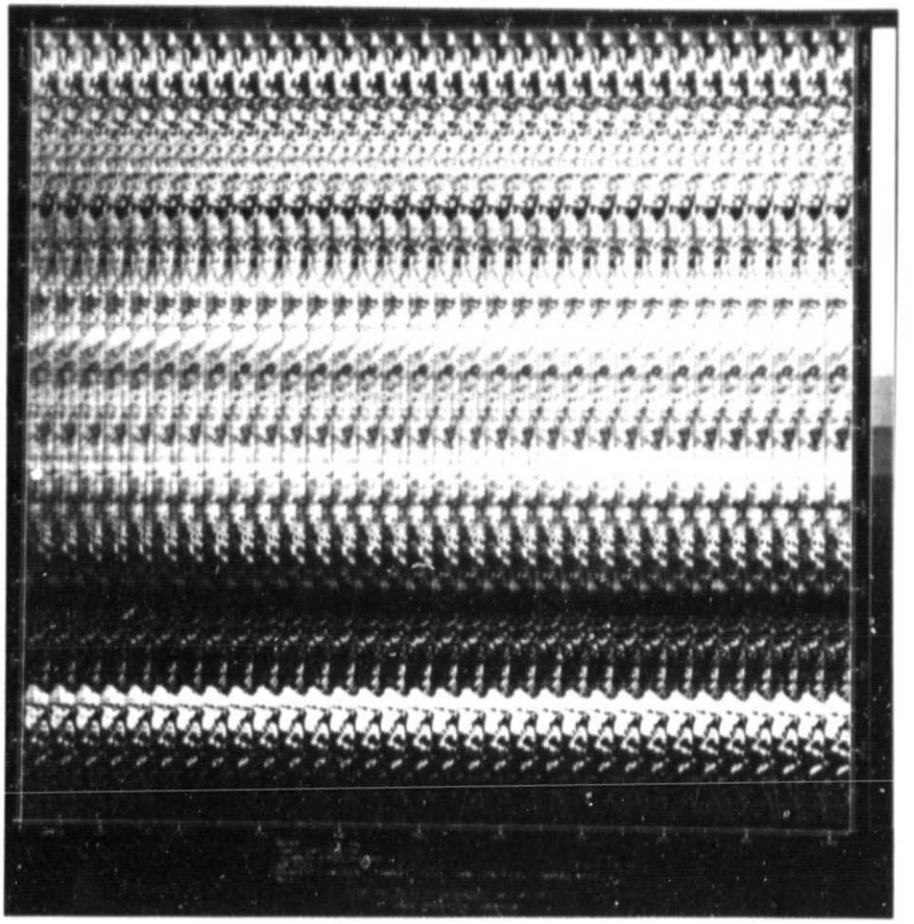

Figure 8a.

Figure 8a is a print of the northern section of the AIS flight for grating position 1. The area of overlap with the center portion of the flightline (Figure 8b) is marked along the right margin. The same area looks very different on the two prints.

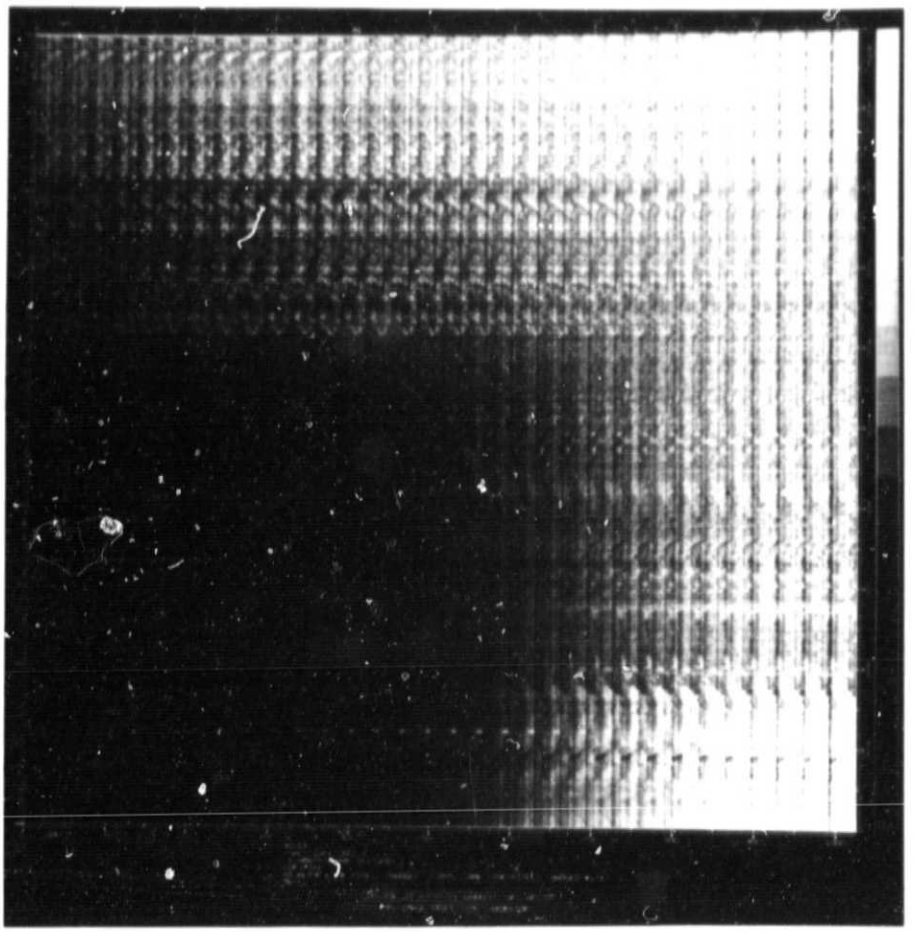

Figure 8b.

Figure 8b is a print of the center section of the AIS flightline for Grating Position 1. Its areas of overlap with both Figure 8a and 8c are marked on the right margin and look considerably different than the same areas in those prints.

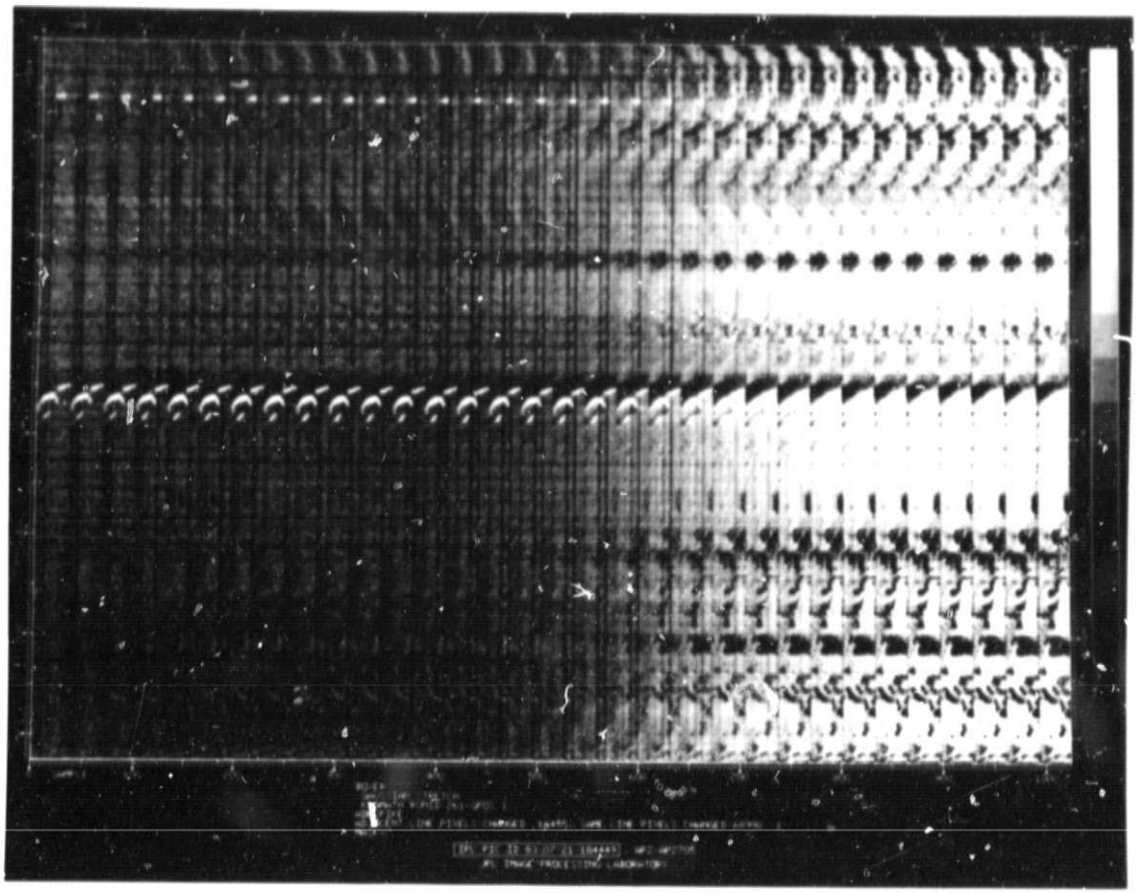

Figure 8c.

Figure 8c is a print of the southern section of the AIS flightline for grating position 1.

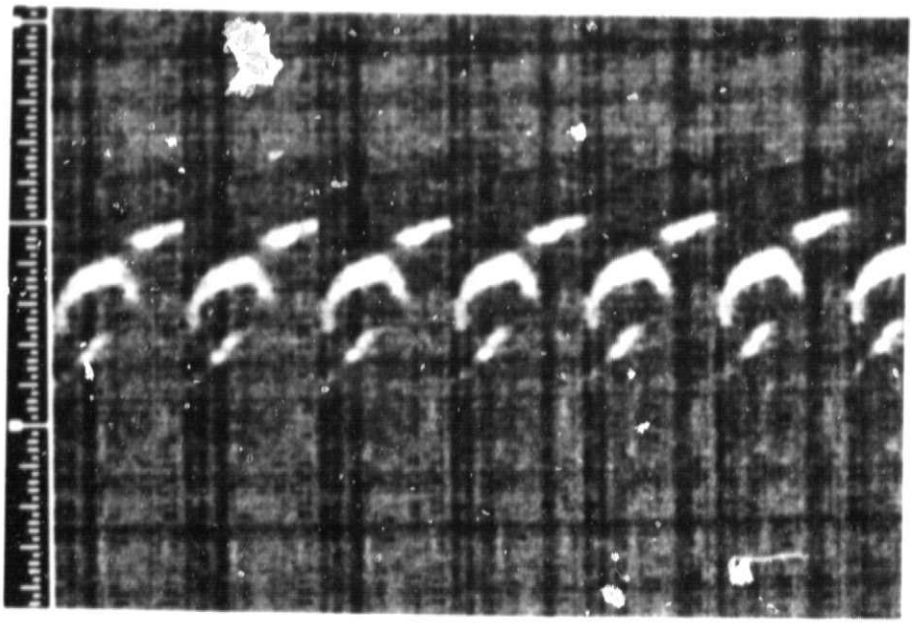

Figure 9a.

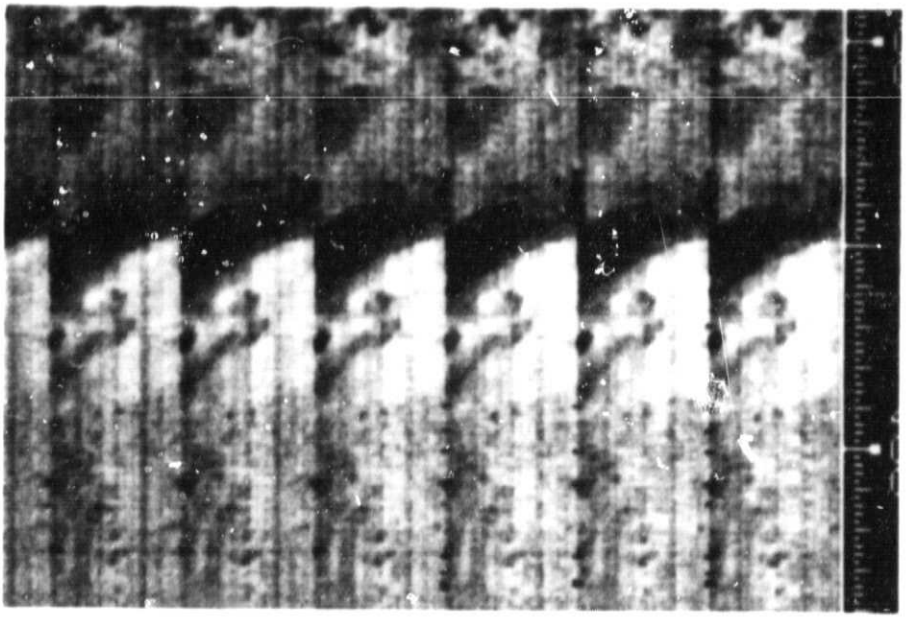

Figure 9b.

Figures 9a and 9b are blowups from the 1.5 and 1.8 ends of the AIS flightline of grating position 1. This portion of the print shows a cinder cone in greater detail.

Figure 10a.

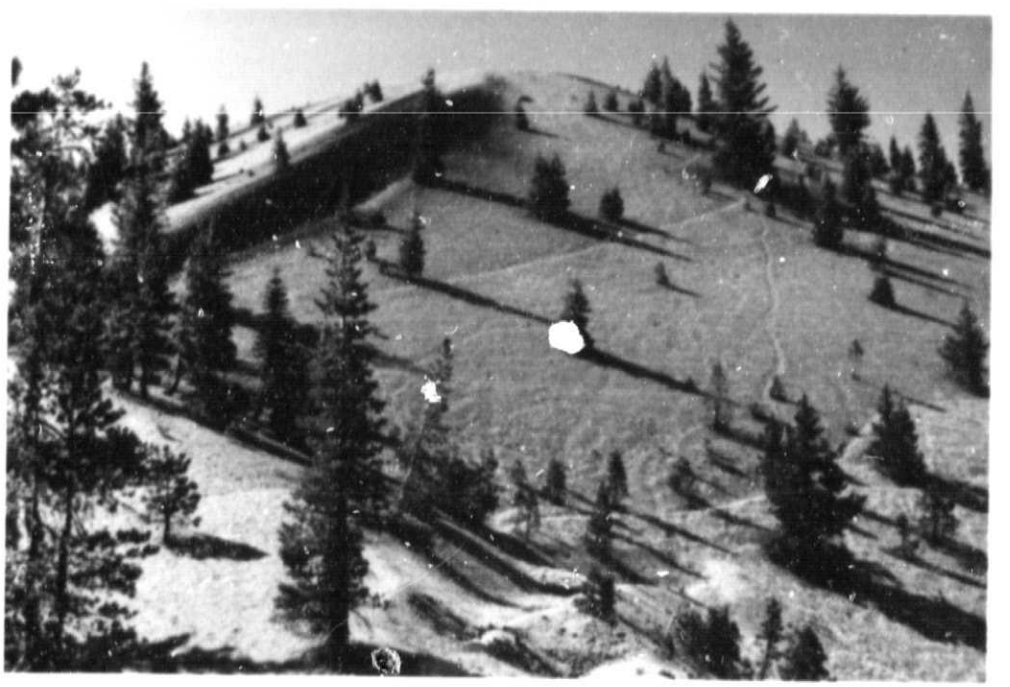

Figure 10b.

Figures 10a and 10b show the general appearance of the cinder cone shown in the AIS imagery in Figures 9a and 9b. Three colors of ejecta are visible in these pictures: white, black, and red.

1

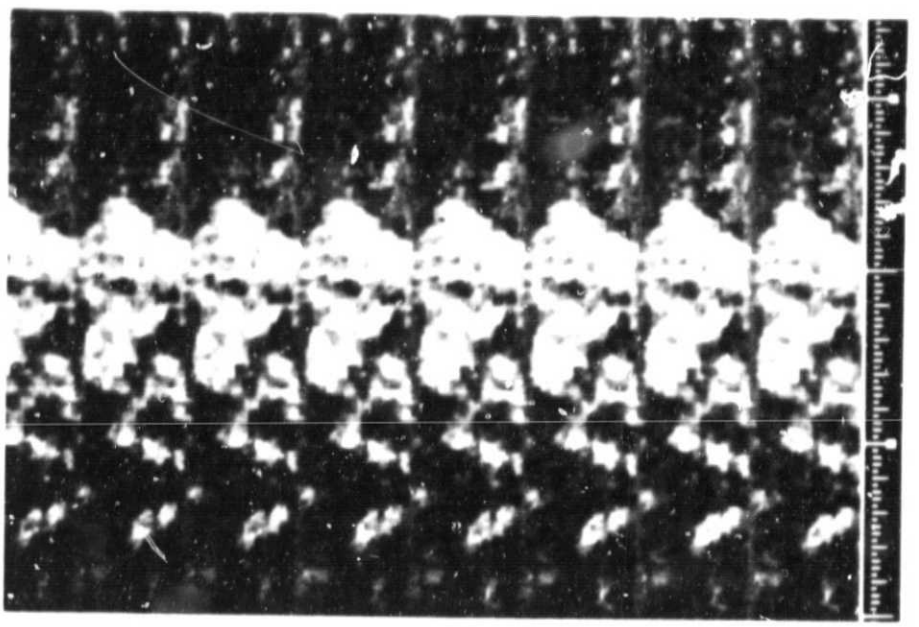

Figure 11.

Figure 11 is a blowup of a portion of the grating position 0 print of the area of scarified soil. This feature is more apparent in the AIS imagery than the panchromatic 35mm print from the onboard Nikon camera (Figure 12).

BLACK AND WHITE PHOTOGRAPH

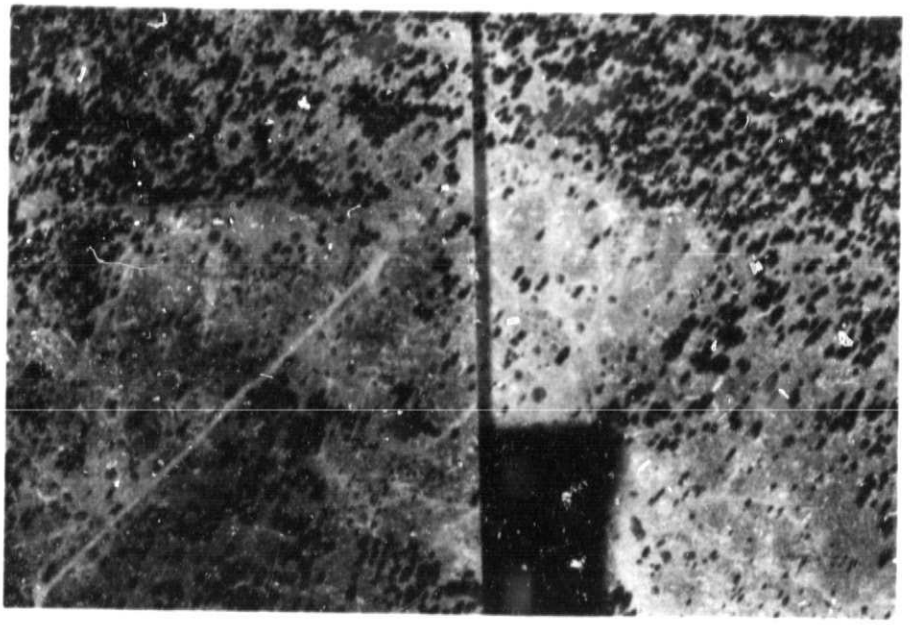

Figure 12.

Figure 12 is a portion of two prints from the onboard Nikon 35mm camera taken during the AIS overpass. This picture corresponds to the area in the AIS print shown in Figure 11. The scarified soil surface is more apparent in the AIS imagery than the 35mm picture sensitive to visible wavelengths.

Figure 13a.

Figure 13b.

Figures 13a and 13b show the scarified soil surface examined in Figures 11 and 12. Figure 13a is a general view of the area, and 13b a closeup of the surface (notice the foot for scale).

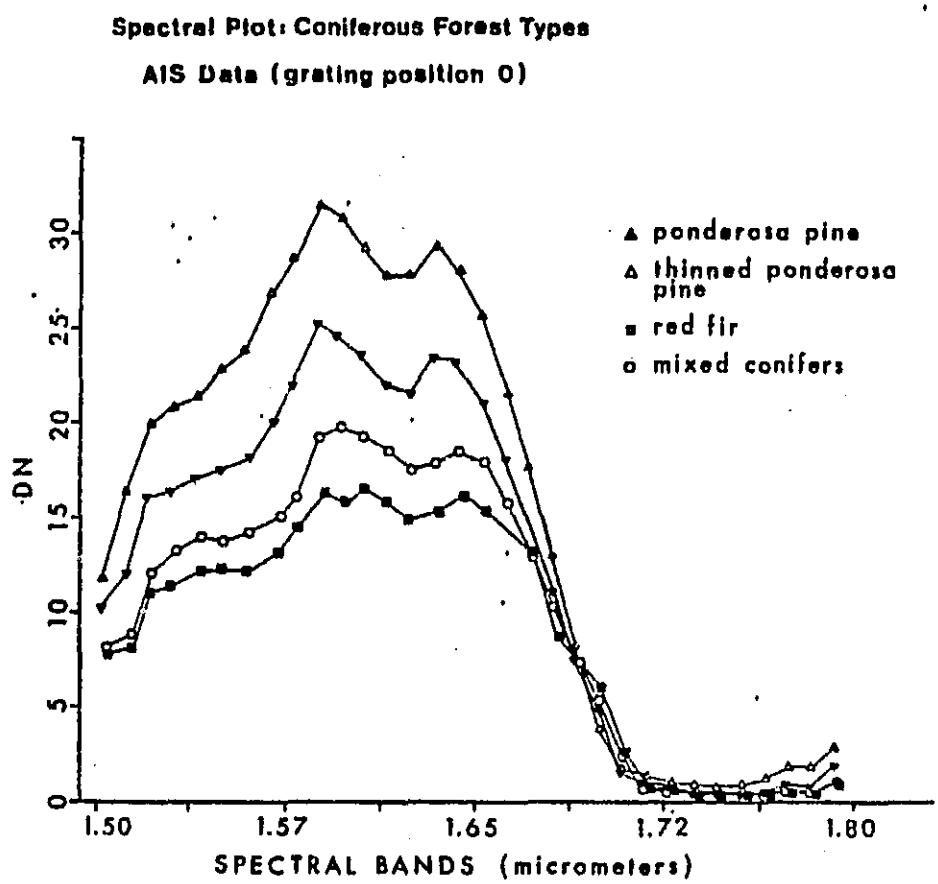

Figure 14.

Figure 14 plots reflectance in digital counts (DNs) as a function of wavelength for four coniferous forest areas for grating position 0.

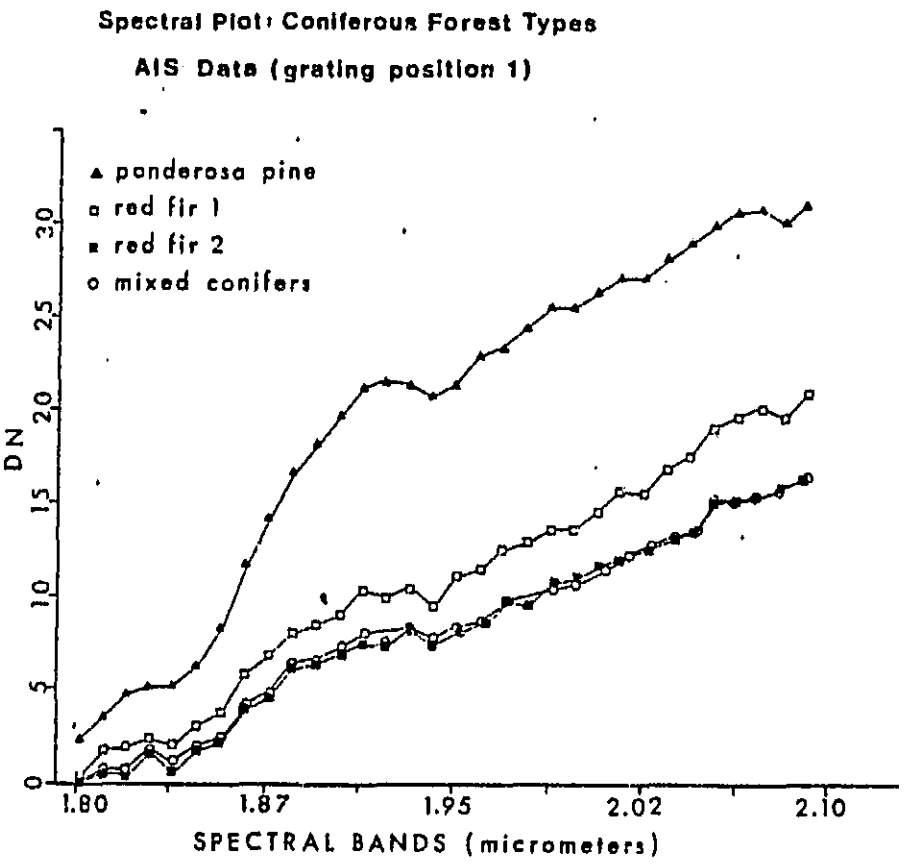

Figure 15.

Figure 15 shows a plot of reflectance in digital counts (DNs) as a function of wavelength for grating position 1 for four coniferous forest areas.